

Hyperfine Quenching of the $4s4p\ ^3P_0$ Level in Zn-like Ions

J. P. Marques¹, F. Parente², and P. Indelicato³

¹ Centro de Física Atómica e Departamento Física, Faculdade de Ciências, Universidade de Lisboa, Campo Grande, Ed. C8, 1749-016 Lisboa, Portugal, e-mail: jmmarques@fc.ul.pt

² Centro de Física Atómica da Universidade de Lisboa e Departamento Física da Faculdade de Ciências e Tecnologia da Universidade Nova de Lisboa, Monte da Caparica, 2825-114 Caparica, Portugal, e-mail: facp@fct.unl.pt

³ Laboratoire Kastler Brossel, École Normale Supérieure; CNRS; Université P. et M. Curie - Paris 6
Case 74; 4, place Jussieu, 75252 Paris CEDEX 05, France, e-mail: paul.indelicato@spectro.jussieu.fr

Received: October 24, 2018/ Revised version: date

Abstract. In this paper, we used the multiconfiguration Dirac-Fock method to compute with high precision the influence of the hyperfine interaction on the $[Ar]3d^{10}4s4p\ ^3P_0$ level lifetime in Zn-like ions for stable and some quasi-stable isotopes of nonzero nuclear spin between $Z = 30$ and $Z = 92$. The influence of this interaction on the $[Ar]3d^{10}4s4p\ ^3P_1 - [Ar]3d^{10}4s4p\ ^3P_0$ separation energy is also calculated for the same ions.

PACS. 31.30.Gs – 31.30.Jv – 32.70.Cs

1 Introduction

It has been found before that the hyperfine interaction plays a fundamental role in the lifetimes and energy separations of the 3P_0 and 3P_1 levels of the configurations $1s2p$ in He-like [1, 2, 3, 4, 5, 6, 7, 8, 9], $[He]2s2p$ in Be-like [10, 11, 12], and $[Ne]3s3p$ in Mg-like [11, 13] ions, and also in $3d^4J = 4$ level in the Ti-like ions [14].

In the He-like ions, in the region $Z \approx 45$, these two levels undergo a level crossing [15] and are nearly degenerate due to the electron-electron magnetic interaction, which leads to a strong influence of the hyperfine interaction on the energy splitting and on the 3P_0 lifetime for isotopes with nonzero nuclear spin. In Be-like, Mg-like and Zn-like ions a level crossing of the 3P_0 and 3P_1 levels has not been found [16], but hyperfine interaction still has strong influence on the lifetime of the 3P_0 metastable level and on the energy splitting, for isotopes with nonzero nuclear spin.

Until recently, laboratory measurements of atomic metastable states hyperfine quenching have been performed only for He-like systems, for $Z = 28$ to $Z = 79$ [3, 4, 5, 8, 17, 18, 19, 20]. Hyperfine-induced transition lines in Be-like systems have been found in the planetary nebula NGC3918 [12]. Measured values of transition probabilities were found to agree with computed values [11, 21].

Divalent atoms are being investigated, both theoretically and experimentally, in order to investigate the possible use of the hyperfine quenched 3P_0 metastable state for ultraprecise optical clocks and trapping experiments [22].

Recently, dielectronic recombination rate coefficients were measured for three isotopes of Zn-like Pt^{48+} in the

Heidelberg heavy-ion storage ring TSR [23]. It was suggested that hyperfine quenching of the $4s4p\ ^3P_0$ in isotopes with non-zero nuclear spin could explain the differences detected in the observed spectra.

In this paper we extend our previous calculations [2, 10, 13] to the influence of the hyperfine interaction on the $1s^22s^22p^63s^23p^63d^{10}4s4p$ levels in Zn-like ions.

In Fig. 1 we show the energy level scheme, not to scale, of these ions. The 3P_0 level is a metastable level; one-photon transitions from this level to the ground state are forbidden, and multiphoton transitions have been found to be negligible in similar systems, so the same behavior can be expected for Zn-like ions. Therefore, in first approximation, we will consider the lifetime of this level as infinite. The energy separation between the $4\ ^3P_0$ and $4\ ^3P_1$ levels is small for Z values around the neutral Zn atom and increases very rapidly with Z . Hyperfine interaction is expected to have a strong influence on the energy splitting and on the $4\ ^3P_0$ lifetime for isotopes with nonzero nuclear spin.

The different steps of this calculation are described in Refs. [2, 24]. Here we will emphasize only the fundamental topics of the theory and the characteristic features of Zn-like systems.

In this work we used the multi-configuration Dirac-Fock code of Desclaux and Indelicato [25, 26, 27] to evaluate, completely *ab initio* the $4s4p$ fine structure energies and transition probabilities.

Several terms, such as the nonrelativistic (J independent) contribution to the correlation, are the same for all levels. In this calculation Breit interaction is included, as well as radiative corrections, using the method described,

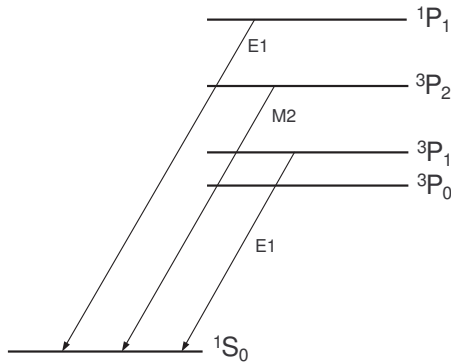


Fig. 1. Energy level and transition scheme for Zn-like ions (not to scale).

for instance, in Ref. [28] and references therein. The MCDF method, in principle, allows for precise calculations because it can include most of the correlation relatively easily, i. e., with a small number of configurations. Here, correlation is important in the determination of transition energies to the ground state, which are used in the calculation of transition probabilities. We found that the largest effect is obtained by using $[\text{Ar}]3d^{10}4s^2$ and $4p^2$ as the configuration set for the ground state. For the excited states we included all configuration state functions (CSF) originated from $[\text{Ar}]3d^{10}4s4p$, $4p4d$, and $4d4f$ (which is usually defined as intrashell correlation), because in second-order perturbation theory the dominant energy difference denominators correspond to these configurations. Correlation originating from interaction with the Ar-like core has been neglected. In particular we included, in a test calculation, spin-polarization from s subshells and found a negligible influence in both energies and transition probabilities. We note that the fine structure energy separation, $\Delta E_{0;fs} = E_{3P_1} - E_{3P_0}$, which is the important parameter in the calculation of the hyperfine quenching, is not very sensitive to correlation, similarly to what we found for systems with smaller number of electrons [10,13]. The same set of CSF have been used for energy, transition probabilities, and for the calculation of the hyperfine matrix elements.

All energy calculations are done in the Coulomb gauge for the retarded part of the electron-electron interaction, to avoid spurious contributions (see for example Refs. [29, 31]). The lifetime calculations are all done using exact relativistic formulas. The length gauge has been used for all transition probabilities.

2 Relativistic calculation of hyperfine contribution to fine structure splitting and to transition probabilities

In the case of a nucleus with nonzero spin, the hyperfine interaction between the nucleus and the electrons must be taken into account. The correspondent Hamiltonian can

be written as

$$H_{\text{hfs}} = \sum_k \mathbf{M}^{(k)} \cdot \mathbf{T}^{(k)}, \quad (1)$$

where $\mathbf{M}^{(k)}$ and $\mathbf{T}^{(k)}$ are spherical tensors of rank k , representing, respectively, the nuclear and the atomic parts of the interaction. As in the case of He-like, Be-like and Mg-like ions, the only sizable contribution from Eq. (1) is the magnetic dipole term ($k = 1$). The hyperfine interaction mixes states with the same $F = J + I$ values. In our case, we are interested in the 3P_0 level, so $J = 0$ and $F = I$. The contribution of this interaction for the total energy has been evaluated through the diagonalization of the matrix:

$$H_{\text{tot}} = \begin{bmatrix} E_0 + \frac{1}{2}i\Gamma_0 + W_{0,0} & W_{0,1} & W_{0,2} \\ W_{1,0} & E_1 + \frac{1}{2}i\Gamma_1 + W_{1,1} & W_{1,2} \\ W_{2,0} & W_{2,1} & E_2 + \frac{1}{2}i\Gamma_2 + W_{2,2} \end{bmatrix} \quad (2)$$

Here, E_f is the unperturbed level energy and Γ_f is the radiative width of the unperturbed level ($f = 0, 1, 2$ stands, respectively, for $^3P_0, ^3P_1, ^1P_1$). In reality there is a fourth level, 3P_2 , which we included in all calculations but was found unnecessary, because the influence of this level in the 3P_0 lifetime is negligible. This can be explained by the large energy separation between the 3P_2 and 3P_0 levels and also because the probability of the allowed M2 transition $4s4p\ ^3P_2 \rightarrow 4s^2\ ^1S_0$ is many orders of magnitude smaller than those of the E1 transitions $4s4p\ ^3P_1 \rightarrow 4s^2\ ^1S_0$ and $4s4p\ ^1P_1 \rightarrow 4s^2\ ^1S_0$. Also, the magnetic dipole hyperfine matrix element between the 3P_2 and 3P_0 levels is very small. This also leads to a negligible influence of the 3P_2 level on the $^3P_1 - ^3P_0$ separation energy. This is consistent with the results of Plante e Johnson [32], who found that the magnetic quadrupole term of the hyperfine interaction affects the 3P_2 level only at high Z . The influence of the 1P_1 level, however, must be taken into account, specially for light nuclei, because the large energy separation between 1P_1 and 3P_0 levels is compensated by the much shorter lifetime of the 1P_1 level. The

hyperfine matrix element

$$W_{f,f'} = W_{f',f} = \langle [\text{Ar}] 3d^{10}4s4p f | H_{\text{hfs}} | [\text{Ar}] 3d^{10}4s4p f' \rangle$$

may be written as

$$W_{J_1, J_2} = \langle I, J_1, F, M_F | \mathbf{M}^{(1)} \cdot \mathbf{T}^{(1)} | I, J_2, F, M_F \rangle, \quad (3)$$

where I is the nuclear spin and F the total angular momentum of the atom, and may be put in the form:

$$W_{J_1, J_2} = (-1)^{I+J_1+F} \begin{Bmatrix} I & J_1 & F \\ J_2 & I & 1 \end{Bmatrix} \times \langle I || \mathbf{M}^{(1)} || I \rangle \langle J_1 || \mathbf{T}^{(1)} || J_2 \rangle. \quad (4)$$

The $6j$ symbol leads to $W_{0,0} = 0$. Also the nuclear magnetic moment μ_I in units of the nuclear magneton μ_N may be defined by

$$\mu_I \mu_N = \langle I || \mathbf{M}^{(1)} || I \rangle \begin{pmatrix} I & 1 & I \\ -I & 0 & I \end{pmatrix}, \quad (5)$$

with $\mu_N = eh/2\pi m_p c$.

The electronic matrix elements were evaluated on the basis set $|^3P_0\rangle$, $|^3P_1\rangle$, $|^1P_1\rangle$ with all intrashell correlation included.

The final result is then obtained by a diagonalization of the 3×3 matrix in Eq. (2), the real part of each eigenvalue being the energy of the correspondent level and the imaginary part its lifetime.

3 Results and discussion

The MCDF method has been used to evaluate the influence of the hyperfine interaction on the $[\text{Ar}]3d^{10}4s4p\ ^3P_0$, 3P_1 and 1P_1 levels for all Z values between 30 and 92 and for all stable and some quasi-stable isotopes of nonzero nuclear spin. Contributions from other levels have been found to be negligible. A detailed list of the contributions to the theoretical 3P_0 , 3P_1 and 1P_1 level energies is presented in Table 1, for $Z = 36, 54$, and 82 .

In Table 2 we present, for all possible values of the nuclear spin I , Z , and the mass number A , the diagonal and off-diagonal hyperfine matrix elements $W_{i,j}$, and the nuclear magnetic moment, μ_I [37], in nuclear magneton units. The indexes 0, 1, and 2 in the hyperfine matrix elements stand for 3P_0 , 3P_1 , and 1P_1 , respectively.

In Table 3 are presented, for all possible values of I , Z , and A , the unperturbed separation energies $\Delta E_0 = E_{^3P_1} - E_{^3P_0}$, the hyperfine-affected separation energy ΔE_{hf} , the $4s4p\ ^3P_1$ and $4s4p\ ^1P_1$ levels lifetime values, τ_1 and τ_2 , respectively, which are not affected, within the precision shown, by the hyperfine interaction, and finally the perturbed lifetime τ_0 of the $4s4p\ ^3P_0$ level. As we pointed out before, the unperturbed value of τ_0 is assumed to be infinite.

In Fig. 2 is plotted the difference $E = \Delta E_{\text{hf}} - \Delta E_0$ as a function of Z for the different possible values of nuclear spin. The influence of the hyperfine interaction on this

energy is shown to increase slowly with Z , the increase becoming more rapid for $Z \gtrsim 60$.

In Fig. 3 is plotted the perturbed $4s4p\ ^3P_0$ level lifetime τ_0 , for the different nuclear spin values I , as a function of Z . One can easily conclude that the opening of a new channel for the decay of the $4s4p\ ^3P_0$ level has a dramatic effect on its lifetime.

After submitting this paper, it was brought to our attention the work by Liu *et al* [38], which contains independent calculations of the hyperfine quenched lifetime of the 3P_0 level in several Zn-like ions. Our results for this lifetime are three times higher than the values found by Liu *et al* for $Z = 30$ and 1.5 higher at $Z = 47$. To look for the origin of this discrepancy we used the $^3P_1 \rightarrow ^1S_0$ and $^1P_1 \rightarrow ^1S_0$ transition energies and probabilities of Liu *et al* to diagonalize the matrix in eq. 2 and obtained results very close to our own calculations. As we do not know the values of the hyperfine matrix elements calculated by Liu *et al*, the reasons for this discrepancy remain unknown.

One of the most interesting practical implication of these calculations comes from the relationship between the $4s4p\ ^3P_0 - 4s4p\ ^3P_1$ levels energy separation and the $4s4p\ ^3P_0$ level lifetime (Eq. 2). As referred in [13] this energy separation can be estimated from a measurement of the hyperfine-quenched $4s4p\ ^3P_0$ lifetime of Zn-like ions with nuclear spin $I \neq 0$. This method has been demonstrated for heliumlike Ni^{26+} [4], Ag^{45+} [3], Gd^{62+} [17] and Au^{77+} [8]. In the Zn-like ions case, as in the corresponding Be-like and Mg-like ions, the situations is different, because, even for the highest Z values, the lifetimes involved are much longer than in heavy heliumlike ions. However, measurements of Be-like hyperfine quenched transition rates have been performed from astrophysical sources [12] and the hyperfine quenching of the Zn-like $^{195}\text{Pt}^{48+}$ ion was observed in the TSR heavy-ion storage-ring [23].

The continuous progress in storage rings, ion sources and ion traps leads us to believe that lifetimes between 0.1 s and 10 μs could be measured, with some accuracy, by directly looking at the light emitted by the ions as a function of time, after the trap has been loaded. Very good vacuum inside the trap is needed, of course, if long lifetimes are to be measured. It remains to be demonstrated that this method is experimentally feasible. Such experiments would be able to provide, for different isotopes, the unperturbed energy separation, because nuclear magnetic moments are well known. This would be an interesting way to test our relativistic calculations.

Acknowledgments

This research was partially supported by the FCT projects POCTI/FAT/50356/2002 and POCTI/0303/2003 (Portugal), financed by the European Community Fund FEDER, and by the French-Portuguese collaboration (PESSOA Program, Contract n $^\circ$ 10721NF). Laboratoire Kastler Brossel is Unité Mixte de Recherche du CNRS n $^\circ$ C8552.

References

1. P. J. Mohr, in *Beam Foil Spectroscopy*, I. Sellin and Pegg Eds. Vol. I, 97 (1976)
2. P. Indelicato, F. Parente, and R. Marrus, *Phys. Rev. A*, **40**, 3505 (1989)
3. R. Marrus, A. Simionovici, P. Indelicato, P. Dietrich, P. Charles, J. P. Briand, K. Finlayson, F. Bosh, P. Liesen, and F. Parente, *Phys. Rev. Lett.* **63**, 502 (1989)
4. R.W. Dunford, C.J. Liu, J. Last, N. Berrah-Mansour, R. Vondrasek, D.A. Church and L.J. Curtis, *Phys. Rev. A* **44**, 764 (1991)
5. A. Simionovici, B. B. Birkett, J. P. Briand, P. Charles, D. D. Dietrich, K. Finlayson, P. Indelicato, P. Liesen, and R. Marrus, *Phys. Rev. A* **48**, 1965 (1993)
6. A. Aboussaïd, M. R. Godefroid, P. Jönsson, and C. Froese Fischer, *Phys. Rev. A* **51**, 2031 (1995)
7. A. V. Volotka, V. M. Shabaev, G. Plunien, G. Soff, V. A. Yerokhin, *Can. J. Phys.* **80**, 1263 (2002)
8. S. Toleikis, B. Manil, E. Berdermann, H. F. Beyer, F. Bosch, M. Czanta, R. W. Dunford, A. Gumberidze, P. Indelicato, C. Kozhuharov, D. Liesen, X. Ma, R. Marrus, P. H. Mokler, D. Schneider, A. Simionovici, Z. Stachura, T. Stöhlker, A. Warczak, Y. Zou, *Phys. Rev. A* **69**, 022507 (2004)
9. W. R. Johnson, K. T. Cheng, D. R. Plante, *Phys. Rev. A* **55**, 2728 (1997)
10. J. P. Marques, F. Parente and P. Indelicato, *Phys. Rev. A* **47**, 929 (1993)
11. T. Brage, P. G. Judge, A. Aboussaïd, M. Godefroid, P. Jönsson, A. Ynnerman, C. F. Fischer, and D. S. Leckrone, *Astrophys. J.* **500**, 507 (1998)
12. T. Brage, P. G. Judge, and C. R. Proffitt, *Phys. Rev. Lett.* **89**, 0281101 (2002)
13. J. P. Marques, F. Parente and P. Indelicato, *ADNDT*, **55**, 157 (1993)
14. F. Parente, J. P. Marques and P. Indelicato, *Europhys. Lett.* **26**, 437 (1994)
15. W. R. Johnson and C. D. Lin, *Phys. Rev. A* **14**, 565 (1976)
16. J. P. Marques, Ph.D. Thesis submitted to the University of Lisbon, unpublished (1994)
17. P. Indelicato, B. B. Birkett, J. P. Briand, P. Charles, D. D. Dietrich, R. Marrus, and A. Simionovici, *Phys. Rev. Lett.* **68**, 1307 (1992)
18. R. W. Dunford, H. G. Berry, D. A. Church, M. Hass, C. J. Liu, M. Raphaelian, B. J. Zabransky, L. J. Curtis, A. E. Livingston, *Phys. Rev. A* **48** 2729 (1993)
19. B. B. Birkett, J. P. Briand, P. Charles, D. D. Dietrich, K. Finlayson, P. Indelicato, D. Liesen, R. Marrus, A. Simionovici, *Phys. Rev. A* **47** R2454 (1993)
20. A. Simionovici, B. B. Birkett, R. Marrus, P. Charles, P. Indelicato, D. D. Dietrich, K. Finlayson, *Phys. Rev. A* **49** 3553 (1994)
21. J. P. Marques, F. Parente and P. Indelicato, Abstracts of the XXIV Reunión de la Real Sociedad Española de Física, Vol. 1, 228 (2003)
22. S. G. Porsev and A. Derevianko, *Phys. Rev. A* **69**, 042506 (2004)
23. S. Schippers, G. Gwinner, C. Brandau, S. Böhm, M. Grieser, S. Kieslich, H. Knopp, A. Müller, R. Repnow, D. Schwalm, and A. Wolf, *Nucl. Instrum. Meth. B* **235**, 265 (2005)
24. K. T. Cheng and W. J. Childs, *Phys. Rev. A* **31**, 2775 (1985)
25. J. P. Desclaux, in *Methods and Techniques in Computational Chemistry* (STEF, Cagliari, 1993), Vol. A
26. P. Indelicato, *Phys. Rev. Lett.* **77**, 3323 (1996)
27. MCDFGME, a MultiConfiguration Dirac Fock and General Matrix Elements program, “(release 2006)”, written by J. P. Desclaux and P. Indelicato (<http://dirac.spectro.jussieu.fr/mcdf>)
28. J. P. Santos, G. C. Rodrigues, J. P. Marques, F. Parente, J. P. Desclaux, and P. Indelicato, *Eur. Phys. J. D* **37**, 201 (2006)
29. O. Gorceix and P. Indelicato, *Phys. Rev. A* **37**, 1087 (1988)
30. E. Lindroth and A.-M. Martensson-Pendrill, *Phys. Rev. A* **39**, 3794 (1989)
31. I. Lindgren, *J. Phys. B* **23**, 1085 (1990)
32. W. R. Johnson, K. T. Cheng, D. R. Plante, *Phys. Rev. A* **55**, 2728 (1997)
33. V. A. Yerokhin, P. Indelicato, V. M. Shabaev, *Eur. Phys. J. D* **25**, 203 (2003)
34. V. A. Yerokhin, P. Indelicato, V. M. Shabaev, *Phys. Rev. A* **71**, 40101 (2005)
35. V. A. Yerokhin, P. Indelicato, V. M. Shabaev, *J. Exp. Theor. Phys.* **101**, 280 (2005)
36. P. Mohr, B. N. Taylor, *Rev. Mod. Phys.* **77** 1 (2005)
37. P. Raghavan, *At. Data Nucl. Data Tables* **42**, 189 (1989)
38. Y. Liu, R. Hutton, Y. Zou, M. Andersson, T. Brage, *J. Phys. B* **39** 3147 (2006)

Table 1. Contribution to the energy of the $4s4p\ ^3P_0, ^3P_1$ and 1P_1 levels (in eV).

	3P_0	3P_1	1P_1
		$Z = 36$	
Coulomb [†]	-75616.613	-75616.265	-75609.264
Magnetic [†]	42.785	42.779	42.765
Retardation (order ω^2) [†]	-4.095	-4.095	-4.094
Retardation ($> \omega^2$)	-0.197	-0.197	-0.197
Self-energy (SE)	31.358	31.363	31.366
Self-energy screening	-2.735	-2.740	-2.743
VP [$\alpha(Z\alpha)$]correction to e-e interaction	0.033	0.033	0.033
Vacuum Polarization $\alpha(Z\alpha)^3 + \alpha^2(Z\alpha)$	0.010	0.010	0.010
2nd order (SE-SE + SE-VP + S-VP-E) [‡]	-0.031	-0.031	-0.031
Recoil	-0.003	-0.003	-0.003
Relativistic Recoil [‡]	0.009	0.009	0.009
Total energy	-75549.478	-75549.137	-75542.148
		$Z = 54$	
Coulomb [†]	-195348.063	-195344.974	-195317.667
Magnetic [†]	171.169	171.142	170.943
Retardation (order ω^2) [†]	-17.418	-17.418	-17.417
Retardation ($> \omega^2$)	-1.711	-1.713	-1.731
Self-energy (SE)	127.610	127.615	127.669
Self-energy screening	-9.166	-9.170	-9.205
VP [$\alpha(Z\alpha)$]correction to e-el interaction	0.124	0.124	0.124
Vacuum Polarization $\alpha(Z\alpha)^3 + \alpha^2(Z\alpha)$	0.242	0.242	0.242
2nd order (SE-SE + SE-VP + S-VP-E) [‡]	-0.253	-0.253	-0.253
Recoil	-0.012	-0.012	-0.012
Relativistic Recoil [‡]	0.042	0.042	0.042
Total energy	-195077.437	-195074.376	-195047.265
		$Z = 82$	
Coulomb [†]	-513070.812	-513061.827	-512876.005
Magnetic [†]	710.586	710.511	708.897
Retardation (order ω^2) [†]	-72.655	-72.654	-72.655
Retardation ($> \omega^2$)	-14.666	-14.668	-14.965
Self-energy (SE)	600.177	600.173	600.249
Self-energy screening	-38.198	-38.203	-38.200
VP [$\alpha(Z\alpha)$]correction to e-e interaction	0.572	0.572	0.570
Vacuum Polarization $\alpha(Z\alpha)^3 + \alpha^2(Z\alpha)$	4.192	4.192	4.189
2nd order (SE-SE + SE-VP + S-VP-E) [‡]	-2.975	-2.975	-2.974
Recoil	-0.051	-0.051	-0.051
Relativistic Recoil [‡]	0.191	0.191	0.191
Total energy	-511883.638	-511874.738	-511690.755

[†] Contains the Uehling potential contribution to all order and all order Breit interaction.[‡] Calculated using the results of Ref. [33,34,35].[‡] The formulas and definitions used to evaluate this term are Appendix A of Ref. [36]

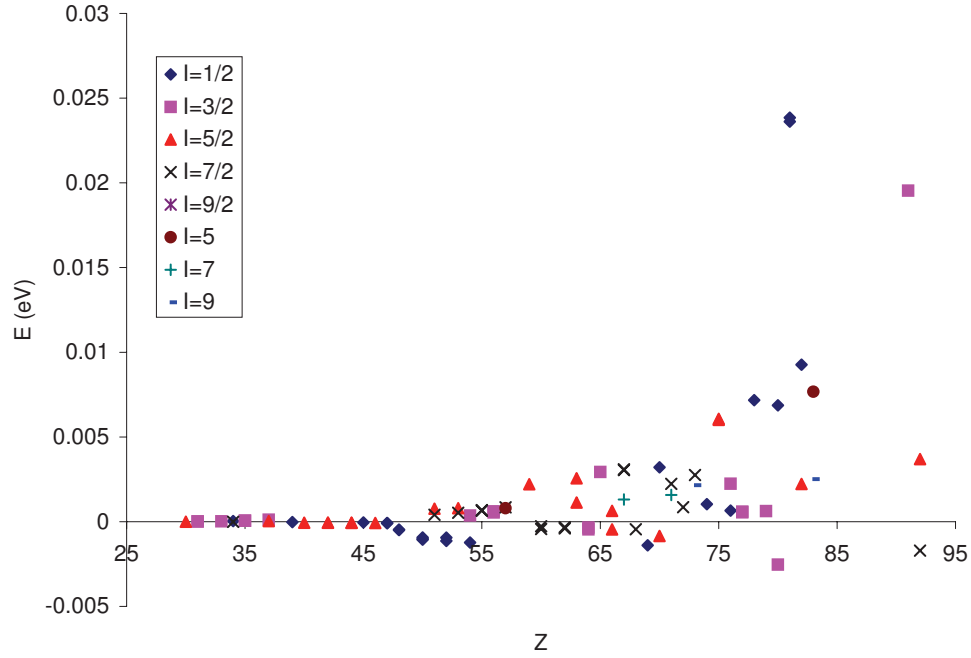


Fig. 2. Influence of the hyperfine interaction on the $4s4p\ ^3P_1 - ^3P_0$ energy separation, as a function of the nuclear spin I and the atomic number Z . The quantity $E = \Delta E_{\text{hf}} - \Delta E_0$ is the contribution of the hyperfine interaction to the fine structure splitting ΔE_0 . The symbols represent values for the different nuclear spins; some elements have several isotopes with identical spins but different μ_I values.

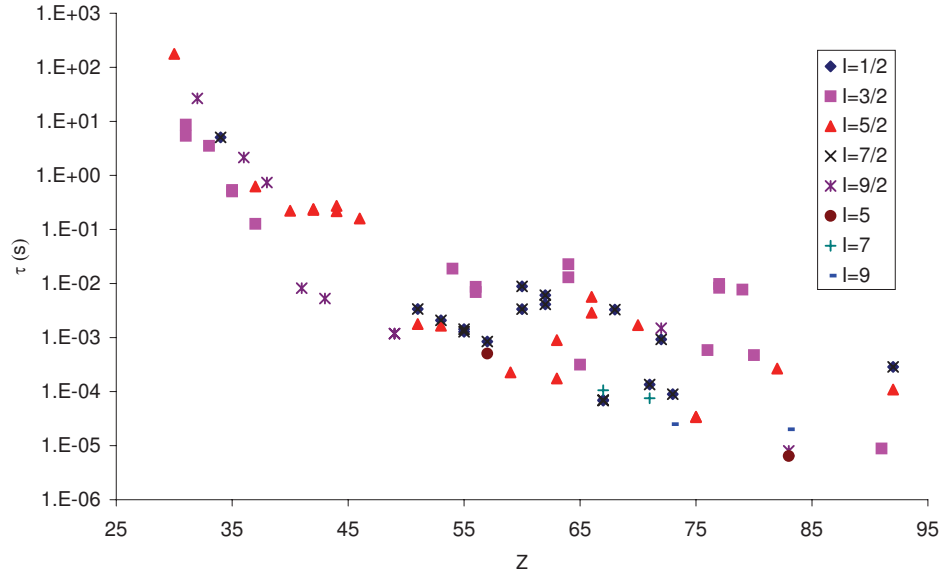


Fig. 3. Influence of the hyperfine interaction on the lifetime of the $4s4p\ ^3P_0$ level, as a function of the nuclear spin I and the atomic number Z . The unperturbed lifetime is, to a very good approximation, infinite.

Table 2. Hyperfine Matrix elements $W_{i,j}$ in eV. The indexes 0, 1, and 2 stand for 3P_0 , 3P_1 , and 1P_1 respectively. I is the nuclear spin and μ the nuclear magnetic moment in nuclear magneton units.

I	Z	A	$W_{1,1}$	$W_{2,2}$	$W_{0,1}$	$W_{0,2}$	$W_{1,2}$	μ_I	
1/2	34	77	-3.312×10^{-05}	-3.245×10^{-06}	-2.382×10^{-05}	1.708×10^{-05}	3.268×10^{-05}	0.535042	
	39	89	2.697×10^{-05}	4.139×10^{-07}	1.670×10^{-05}	-1.055×10^{-05}	-2.199×10^{-05}	-0.137415	
	45	103	4.648×10^{-05}	-4.491×10^{-06}	2.564×10^{-05}	-1.321×10^{-05}	-2.923×10^{-05}	-0.0884	
	47	107	7.878×10^{-05}	-1.013×10^{-05}	4.218×10^{-05}	-2.011×10^{-05}	-4.507×10^{-05}	-0.11368	
	47	109	9.057×10^{-05}	-1.164×10^{-05}	4.849×10^{-05}	-2.311×10^{-05}	-5.182×10^{-05}	-0.130691	
	48	111	4.696×10^{-04}	-6.718×10^{-05}	2.480×10^{-04}	-1.136×10^{-04}	-2.560×10^{-04}	-0.594886	
	48	113	4.912×10^{-04}	-7.027×10^{-05}	2.594×10^{-04}	-1.188×10^{-04}	-2.678×10^{-04}	-0.622301	
	50	115	9.289×10^{-04}	-1.573×10^{-04}	4.788×10^{-04}	-2.018×10^{-04}	-4.591×10^{-04}	-0.91883	
	50	117	1.012×10^{-03}	-1.714×10^{-04}	5.216×10^{-04}	-2.199×10^{-04}	-5.002×10^{-04}	-1.00104	
	50	119	1.059×10^{-03}	-1.793×10^{-04}	5.457×10^{-04}	-2.301×10^{-04}	-5.233×10^{-04}	-1.04728	
	52	123	9.385×10^{-04}	-1.801×10^{-04}	4.734×10^{-04}	-1.834×10^{-04}	-4.199×10^{-04}	-0.736948	
	52	125	1.132×10^{-03}	-2.172×10^{-04}	5.708×10^{-04}	-2.212×10^{-04}	-5.063×10^{-04}	-0.888505	
	54	129	1.232×10^{-03}	-2.602×10^{-04}	6.102×10^{-04}	-2.170×10^{-04}	-4.984×10^{-04}	-0.777976	
	69	169	1.391×10^{-03}	-3.983×10^{-04}	6.364×10^{-04}	-1.217×10^{-04}	-2.710×10^{-04}	-0.231	
	70	171	-3.210×10^{-03}	9.272×10^{-04}	-1.463×10^{-03}	2.694×10^{-04}	5.974×10^{-04}	0.49367	
	74	183	-1.035×10^{-03}	3.081×10^{-04}	-4.659×10^{-04}	7.391×10^{-05}	1.610×10^{-04}	0.117785	
	76	187	-6.581×10^{-04}	1.982×10^{-04}	-2.942×10^{-04}	4.344×10^{-05}	9.378×10^{-05}	0.064652	
	78	195	-7.176×10^{-03}	2.186×10^{-03}	-3.189×10^{-03}	4.387×10^{-04}	9.383×10^{-04}	0.60952	
	80	199	-6.867×10^{-03}	2.112×10^{-03}	-3.030×10^{-03}	3.892×10^{-04}	8.250×10^{-04}	0.505885	
	81	203	-2.364×10^{-02}	7.305×10^{-03}	-1.040×10^{-02}	1.290×10^{-03}	2.724×10^{-03}	1.622258	
	81	205	-2.387×10^{-02}	7.377×10^{-03}	-1.050×10^{-02}	1.303×10^{-03}	2.751×10^{-03}	1.638215	
	82	207	-9.267×10^{-03}	2.876×10^{-03}	-4.060×10^{-03}	4.873×10^{-04}	1.024×10^{-03}	0.592583	
	3/2	31	69	-1.363×10^{-05}	-1.123×10^{-06}	-2.652×10^{-05}	2.024×10^{-05}	1.535×10^{-05}	2.01659
		31	71	-1.732×10^{-05}	-1.427×10^{-06}	-3.370×10^{-05}	2.572×10^{-05}	1.950×10^{-05}	2.56227
		33	75	-2.179×10^{-05}	-2.286×10^{-06}	-3.670×10^{-05}	2.687×10^{-05}	2.235×10^{-05}	1.43948
		35	79	-5.715×10^{-05}	-4.904×10^{-06}	-8.849×10^{-05}	6.206×10^{-05}	5.431×10^{-05}	2.1064
		35	81	-6.161×10^{-05}	-5.286×10^{-06}	-9.538×10^{-05}	6.690×10^{-05}	5.855×10^{-05}	2.270562
		37	87	-1.198×10^{-04}	-6.370×10^{-06}	-1.745×10^{-04}	1.165×10^{-04}	1.056×10^{-04}	2.75131
54		131	-3.649×10^{-04}	7.708×10^{-05}	-4.042×10^{-04}	1.438×10^{-04}	1.477×10^{-04}	0.6915	
56		135	-5.429×10^{-04}	1.235×10^{-04}	-5.920×10^{-04}	1.932×10^{-04}	1.987×10^{-04}	0.837953	
56		137	-6.073×10^{-04}	1.382×10^{-04}	-6.622×10^{-04}	2.161×10^{-04}	2.222×10^{-04}	0.937365	
64		155	3.449×10^{-04}	-9.328×10^{-05}	3.595×10^{-04}	-8.381×10^{-05}	-8.504×10^{-05}	-0.2572	
64		157	4.556×10^{-04}	-1.232×10^{-04}	4.750×10^{-04}	-1.107×10^{-04}	-1.123×10^{-04}	-0.3398	
65		159	-2.936×10^{-03}	8.052×10^{-04}	-3.049×10^{-03}	6.825×10^{-04}	6.901×10^{-04}	2.014	
76		189	-2.239×10^{-03}	6.745×10^{-04}	-2.238×10^{-03}	3.305×10^{-04}	3.191×10^{-04}	0.659933	
77		191	-5.500×10^{-04}	1.666×10^{-04}	-5.481×10^{-04}	7.811×10^{-05}	7.506×10^{-05}	0.1507	
77		193	-5.974×10^{-04}	1.810×10^{-04}	-5.954×10^{-04}	8.484×10^{-05}	8.154×10^{-05}	0.1637	
79		197	-6.243×10^{-04}	1.911×10^{-04}	-6.182×10^{-04}	8.215×10^{-05}	7.824×10^{-05}	0.148158	
80		201	2.535×10^{-03}	-7.798×10^{-04}	2.501×10^{-03}	-3.212×10^{-04}	-3.045×10^{-04}	-0.560226	
91		231	-1.960×10^{-02}	6.265×10^{-03}	-1.845×10^{-02}	1.656×10^{-03}	1.506×10^{-03}	2.01	
5/2		30	67	-1.975×10^{-06}	-3.436×10^{-08}	-6.734×10^{-06}	5.115×10^{-06}	2.303×10^{-06}	0.875479
		37	85	-3.537×10^{-05}	-1.880×10^{-06}	-7.865×10^{-05}	5.252×10^{-05}	3.118×10^{-05}	1.353352
	40	91	6.158×10^{-05}	-2.554×10^{-07}	1.273×10^{-04}	-7.804×10^{-05}	-4.821×10^{-05}	-1.30362	
	42	95	6.081×10^{-05}	-2.597×10^{-06}	1.207×10^{-04}	-6.931×10^{-05}	-4.375×10^{-05}	-0.9142	
	42	97	6.209×10^{-05}	-2.652×10^{-06}	1.233×10^{-04}	-7.078×10^{-05}	-4.467×10^{-05}	-0.9335	
	44	99	5.826×10^{-05}	-4.623×10^{-06}	1.116×10^{-04}	-5.968×10^{-05}	-3.835×10^{-05}	-0.6413	
	44	101	6.530×10^{-05}	-5.182×10^{-06}	1.251×10^{-04}	-6.689×10^{-05}	-4.298×10^{-05}	-0.7188	
	46	105	7.773×10^{-05}	-8.788×10^{-06}	1.442×10^{-04}	-7.151×10^{-05}	-4.664×10^{-05}	-0.642	
	51	121	-7.648×10^{-04}	1.385×10^{-04}	-1.332×10^{-03}	5.382×10^{-04}	3.597×10^{-04}	3.3634	
	53	127	-8.004×10^{-04}	1.617×10^{-04}	-1.366×10^{-03}	5.072×10^{-04}	3.406×10^{-04}	2.813273	
	59	141	-2.218×10^{-03}	5.482×10^{-04}	-3.622×10^{-03}	1.040×10^{-03}	6.985×10^{-04}	4.2754	
	63	151	-2.567×10^{-03}	6.842×10^{-04}	-4.106×10^{-03}	9.970×10^{-04}	6.642×10^{-04}	3.4717	
	63	153	-1.133×10^{-03}	3.020×10^{-04}	-1.812×10^{-03}	4.401×10^{-04}	2.932×10^{-04}	1.5324	
	66	161	4.556×10^{-04}	-1.264×10^{-04}	7.196×10^{-04}	-1.548×10^{-04}	-1.021×10^{-04}	-0.4803	
	66	163	-6.384×10^{-04}	1.771×10^{-04}	-1.008×10^{-03}	2.169×10^{-04}	1.431×10^{-04}	0.673	
	70	173	8.428×10^{-04}	-2.434×10^{-04}	1.312×10^{-03}	-2.416×10^{-04}	-1.568×10^{-04}	-0.648	
	75	185	-6.034×10^{-03}	1.807×10^{-03}	-9.246×10^{-03}	1.415×10^{-03}	8.981×10^{-04}	3.1871	
	75	187	-6.096×10^{-03}	1.826×10^{-03}	-9.341×10^{-03}	1.429×10^{-03}	9.073×10^{-04}	3.2197	
82	205	-2.226×10^{-03}	6.908×10^{-04}	-3.331×10^{-03}	3.998×10^{-04}	2.460×10^{-04}	0.7117		
92	233	1.702×10^{-03}	-5.451×10^{-04}	3.263×10^{-03}	-2.839×10^{-04}	-1.256×10^{-04}	0.59		

Table 2. *Continued*

I	Z	A	$W_{1,1}$	$W_{2,2}$	$W_{0,1}$	$W_{0,2}$	$W_{1,2}$	μ_I	
7/2	34	79	9.003×10^{-06}	8.821×10^{-07}	2.967×10^{-05}	-2.128×10^{-05}	-8.883×10^{-06}	-1.018	
	51	123	-4.141×10^{-04}	7.500×10^{-05}	-9.673×10^{-04}	3.910×10^{-04}	1.948×10^{-04}	2.5498	
	53	129	-5.326×10^{-04}	1.076×10^{-04}	-1.220×10^{-03}	4.528×10^{-04}	2.267×10^{-04}	2.621	
	55	133	-6.480×10^{-04}	1.424×10^{-04}	-1.459×10^{-03}	4.970×10^{-04}	2.494×10^{-04}	2.582025	
	55	135	-6.857×10^{-04}	1.507×10^{-04}	-1.544×10^{-03}	5.260×10^{-04}	2.639×10^{-04}	2.7324	
	57	139	-8.527×10^{-04}	2.001×10^{-04}	-1.892×10^{-03}	5.915×10^{-04}	2.968×10^{-04}	2.783046	
	60	143	4.324×10^{-04}	-1.093×10^{-04}	9.424×10^{-04}	-2.593×10^{-04}	-1.296×10^{-04}	-1.065	
	60	145	2.664×10^{-04}	-6.731×10^{-05}	5.805×10^{-04}	-1.597×10^{-04}	-7.984×10^{-05}	-0.656	
	62	147	3.935×10^{-04}	-1.032×10^{-04}	8.483×10^{-04}	-2.147×10^{-04}	-1.069×10^{-04}	-0.812	
	62	149	3.235×10^{-04}	-8.486×10^{-05}	6.975×10^{-04}	-1.765×10^{-04}	-8.790×10^{-05}	-0.6677	
	67	163	-3.107×10^{-03}	8.721×10^{-04}	-6.561×10^{-03}	1.356×10^{-03}	6.644×10^{-04}	4.23	
	67	165	-3.063×10^{-03}	8.598×10^{-04}	-6.467×10^{-03}	1.337×10^{-03}	6.550×10^{-04}	4.17	
	68	167	4.484×10^{-04}	-1.271×10^{-04}	9.431×10^{-04}	-1.875×10^{-04}	-9.150×10^{-05}	-0.56385	
	71	175	-2.238×10^{-03}	6.514×10^{-04}	-4.657×10^{-03}	8.257×10^{-04}	3.979×10^{-04}	2.2323	
	72	177	-8.583×10^{-04}	2.519×10^{-04}	-1.781×10^{-03}	3.041×10^{-04}	1.459×10^{-04}	0.7935	
	73	181	-2.765×10^{-03}	8.176×10^{-04}	-5.722×10^{-03}	9.414×10^{-04}	4.495×10^{-04}	2.3705	
	92	235	-3.699×10^{-03}	1.185×10^{-03}	-5.287×10^{-03}	4.599×10^{-04}	2.731×10^{-04}	-0.38	
	9/2	32	73	3.089×10^{-06}	3.176×10^{-07}	1.419×10^{-05}	-1.060×10^{-05}	-3.306×10^{-06}	-0.879468
		36	83	1.124×10^{-05}	7.920×10^{-07}	4.326×10^{-05}	-2.963×10^{-05}	-1.029×10^{-05}	-0.970669
38		87	1.959×10^{-05}	6.773×10^{-07}	7.138×10^{-05}	-4.640×10^{-05}	-1.662×10^{-05}	-1.093603	
41		93	-1.930×10^{-04}	4.552×10^{-06}	-6.573×10^{-04}	3.901×10^{-04}	1.449×10^{-04}	6.1705	
43		99	-2.464×10^{-04}	1.512×10^{-05}	-8.076×10^{-04}	4.478×10^{-04}	1.696×10^{-04}	5.6847	
49		113	-5.500×10^{-04}	8.617×10^{-05}	-1.648×10^{-03}	7.241×10^{-04}	2.856×10^{-04}	5.5289	
49		115	-5.512×10^{-04}	8.636×10^{-05}	-1.651×10^{-03}	7.257×10^{-04}	2.862×10^{-04}	5.5408	
72		179	5.392×10^{-04}	-1.582×10^{-04}	1.403×10^{-03}	-2.395×10^{-04}	-9.166×10^{-05}	-0.6409	
83		209	-7.663×10^{-03}	2.388×10^{-03}	-1.922×10^{-02}	2.230×10^{-03}	8.126×10^{-04}	4.1103	
5		57	138	-7.965×10^{-04}	1.869×10^{-04}	-2.439×10^{-03}	7.625×10^{-04}	2.772×10^{-04}	3.713646
	83	208	-7.773×10^{-03}	2.422×10^{-03}	-2.146×10^{-02}	2.491×10^{-03}	8.243×10^{-04}	4.633	
7	67	166	-1.322×10^{-03}	3.711×10^{-04}	-5.264×10^{-03}	1.088×10^{-03}	2.827×10^{-04}	3.6	
	71	176	-1.588×10^{-03}	4.624×10^{-04}	-6.233×10^{-03}	1.105×10^{-03}	2.824×10^{-04}	3.169	
9	73	180	-2.189×10^{-03}	6.472×10^{-04}	-1.083×10^{-02}	1.781×10^{-03}	3.558×10^{-04}	4.825	
	83	210	-2.545×10^{-03}	7.929×10^{-04}	-1.217×10^{-02}	1.412×10^{-03}	2.699×10^{-04}	2.73	

Table 3. Influence of the hyperfine interaction on the $4s4p\ ^3P_1 - 4s4p\ ^3P_0$ energy separation and on the lifetime of the 3P_0 level, as a function of the nuclear spin I and the atomic number Z . ΔE_0 is the unperturbed energy separation (in eV), and ΔE_{hf} is the perturbed energy (in eV) when the hyperfine interaction is taken into account (the 5 digits do not necessarily represent the accuracy of the calculation - they are intended to show the effect at low Z). τ_0 , τ_1 and τ_2 represent the perturbed lifetimes (in s) of $4s4p\ ^3P_0$, 3P_1 and 1P_1 levels respectively.

I	Z	A	ΔE_0	ΔE_{hf}	τ_1	τ_2	τ_0
1/2	34	77	0.20461	0.20458	2.139×10^{-07}	1.340×10^{-10}	$7.847 \times 10^{+00}$
	39	89	0.61806	0.61809	1.393×10^{-08}	5.025×10^{-11}	$1.317 \times 10^{+01}$
	45	103	1.41748	1.41753	1.976×10^{-09}	2.375×10^{-11}	$5.111 \times 10^{+00}$
	47	107	1.74706	1.74714	1.221×10^{-09}	1.923×10^{-11}	$1.847 \times 10^{+00}$
	47	109	1.74706	1.74715	1.221×10^{-09}	1.923×10^{-11}	$1.397 \times 10^{+00}$
	48	111	1.92132	1.92179	9.804×10^{-10}	1.739×10^{-11}	5.286×10^{-02}
	48	113	1.92132	1.92181	9.804×10^{-10}	1.739×10^{-11}	4.831×10^{-02}
	50	115	2.28581	2.28674	6.623×10^{-10}	1.433×10^{-11}	1.391×10^{-02}
	50	117	2.28581	2.28682	6.623×10^{-10}	1.433×10^{-11}	1.172×10^{-02}
	50	119	2.28581	2.28687	6.623×10^{-10}	1.433×10^{-11}	1.071×10^{-02}
	52	123	2.66778	2.66872	4.673×10^{-10}	1.185×10^{-11}	1.397×10^{-02}
	52	125	2.66778	2.66891	4.673×10^{-10}	1.185×10^{-11}	9.609×10^{-03}
	54	129	3.06295	3.06418	3.425×10^{-10}	9.804×10^{-12}	8.274×10^{-03}
	69	169	6.17717	6.17856	7.752×10^{-11}	2.398×10^{-12}	7.234×10^{-03}
	70	171	6.38647	6.38326	7.246×10^{-11}	2.174×10^{-12}	1.367×10^{-03}
	74	183	7.22323	7.22219	5.650×10^{-11}	1.464×10^{-12}	1.353×10^{-02}
	76	187	7.64172	7.64106	5.051×10^{-11}	1.196×10^{-12}	3.400×10^{-02}
	78	195	8.06074	8.05357	4.545×10^{-11}	9.804×10^{-13}	2.895×10^{-04}
	80	199	8.48051	8.47364	4.115×10^{-11}	7.937×10^{-13}	3.215×10^{-04}
	3/2	81	203	8.69084	8.66722	3.922×10^{-11}	7.194×10^{-13}
81		205	8.69084	8.66699	3.922×10^{-11}	7.194×10^{-13}	2.672×10^{-05}
82		207	8.90152	8.89226	3.745×10^{-11}	6.494×10^{-13}	1.794×10^{-04}
31		69	0.06865	0.06864	4.446×10^{-06}	4.528×10^{-10}	$8.711 \times 10^{+00}$
31		71	0.06865	0.06863	4.446×10^{-06}	4.528×10^{-10}	$5.395 \times 10^{+00}$
33		75	0.14992	0.14990	4.831×10^{-07}	1.808×10^{-10}	$3.524 \times 10^{+00}$
35		79	0.26849	0.26843	1.071×10^{-07}	1.044×10^{-10}	5.357×10^{-01}
35		81	0.26849	0.26843	1.071×10^{-07}	1.044×10^{-10}	4.610×10^{-01}
37		87	0.42429	0.42417	3.448×10^{-08}	6.944×10^{-11}	1.270×10^{-01}
54		131	3.06295	3.06259	3.425×10^{-10}	9.804×10^{-12}	1.883×10^{-02}
56		135	3.46760	3.46706	2.611×10^{-10}	8.197×10^{-12}	8.660×10^{-03}
56		137	3.46760	3.46699	2.611×10^{-10}	8.197×10^{-12}	6.920×10^{-03}
64		155	5.12988	5.13022	1.130×10^{-10}	3.876×10^{-12}	2.277×10^{-02}
64		157	5.12988	5.13034	1.130×10^{-10}	3.876×10^{-12}	1.304×10^{-02}
65		159	5.33938	5.33645	1.041×10^{-10}	3.534×10^{-12}	3.155×10^{-04}
76		189	7.64172	7.63948	5.051×10^{-11}	1.196×10^{-12}	5.872×10^{-04}
77		191	7.85115	7.85060	4.785×10^{-11}	1.081×10^{-12}	9.806×10^{-03}
77		193	7.85115	7.85055	4.785×10^{-11}	1.081×10^{-12}	8.310×10^{-03}
79		197	8.27049	8.26987	4.329×10^{-11}	8.850×10^{-13}	7.729×10^{-03}
80		201	8.48051	8.48305	4.115×10^{-11}	7.937×10^{-13}	4.730×10^{-04}
91	231	10.82070	10.80116	2.591×10^{-11}	2.538×10^{-13}	8.872×10^{-06}	
5/2	30	67	0.04546	0.04546	1.834×10^{-05}	1.371×10^{-09}	$1.771 \times 10^{+02}$
	37	85	0.42429	0.42425	3.448×10^{-08}	6.944×10^{-11}	6.251×10^{-01}
	40	91	0.72914	0.72920	9.434×10^{-09}	4.348×10^{-11}	2.221×10^{-01}
	42	95	0.97889	0.97895	4.695×10^{-09}	3.344×10^{-11}	2.395×10^{-01}
	42	97	0.97889	0.97895	4.695×10^{-09}	3.344×10^{-11}	2.297×10^{-01}
	44	99	1.26339	1.26345	2.584×10^{-09}	2.646×10^{-11}	2.732×10^{-01}
	44	101	1.26339	1.26346	2.584×10^{-09}	2.646×10^{-11}	2.175×10^{-01}
	46	105	1.57892	1.57900	1.541×10^{-09}	2.132×10^{-11}	1.597×10^{-01}
	51	121	2.47489	2.47413	5.525×10^{-10}	1.302×10^{-11}	1.779×10^{-03}
	53	127	2.86396	2.86316	3.984×10^{-10}	1.079×10^{-11}	1.661×10^{-03}
	59	141	4.08585	4.08364	1.828×10^{-10}	6.211×10^{-12}	2.274×10^{-04}
	63	151	4.92049	4.91793	1.233×10^{-10}	4.274×10^{-12}	1.747×10^{-04}
	63	153	4.92049	4.91936	1.233×10^{-10}	4.274×10^{-12}	8.977×10^{-04}
	66	161	5.54887	5.54933	9.615×10^{-11}	3.205×10^{-12}	5.667×10^{-03}
66	163	5.54887	5.54823	9.615×10^{-11}	3.205×10^{-12}	2.885×10^{-03}	
70	173	6.38647	6.38731	7.246×10^{-11}	2.174×10^{-12}	1.702×10^{-03}	

Table 3. *Continued*

I	Z	A	ΔE_0	ΔE_{hf}	τ_1	τ_2	τ_0
5/2	75	185	7.43246	7.42645	5.348×10^{-11}	1.325×10^{-12}	3.433×10^{-05}
	75	187	7.43246	7.42639	5.348×10^{-11}	1.325×10^{-12}	3.364×10^{-05}
	82	205	8.90152	8.89930	3.745×10^{-11}	6.494×10^{-13}	2.670×10^{-04}
	92	233	11.03725	11.03356	2.506×10^{-11}	2.288×10^{-13}	1.090×10^{-04}
7/2	34	79	0.20461	0.20462	2.139×10^{-07}	1.340×10^{-10}	$5.060 \times 10^{+00}$
	51	123	2.47489	2.47448	5.525×10^{-10}	1.302×10^{-11}	3.371×10^{-03}
	53	129	2.86396	2.86343	3.984×10^{-10}	1.079×10^{-11}	2.084×10^{-03}
	55	133	3.26430	3.26365	2.976×10^{-10}	8.929×10^{-12}	1.435×10^{-03}
	55	135	3.26430	3.26362	2.976×10^{-10}	8.929×10^{-12}	1.281×10^{-03}
	57	139	3.67249	3.67164	2.304×10^{-10}	7.463×10^{-12}	8.424×10^{-04}
	60	143	4.29381	4.29424	1.645×10^{-10}	5.650×10^{-12}	3.350×10^{-03}
	60	145	4.29381	4.29408	1.645×10^{-10}	5.650×10^{-12}	8.830×10^{-03}
	62	147	4.71127	4.71166	1.351×10^{-10}	4.695×10^{-12}	4.108×10^{-03}
	62	149	4.71127	4.71159	1.351×10^{-10}	4.695×10^{-12}	6.075×10^{-03}
	67	163	5.75836	5.75527	8.929×10^{-11}	2.915×10^{-12}	6.802×10^{-05}
	67	165	5.75836	5.75531	8.929×10^{-11}	2.915×10^{-12}	6.999×10^{-05}
	68	167	5.96779	5.96824	8.264×10^{-11}	2.646×10^{-12}	3.294×10^{-03}
	71	175	6.59569	6.59346	6.757×10^{-11}	1.972×10^{-12}	1.350×10^{-04}
	72	177	6.80490	6.80404	6.369×10^{-11}	1.786×10^{-12}	9.241×10^{-04}
	73	181	7.01409	7.01133	5.988×10^{-11}	1.618×10^{-12}	8.953×10^{-05}
	92	235	11.03725	11.03895	2.506×10^{-11}	2.288×10^{-13}	2.864×10^{-04}
9/2	32	73	0.10442	0.10442	1.298×10^{-06}	2.644×10^{-10}	$2.655 \times 10^{+01}$
	36	83	0.34167	0.34168	5.882×10^{-08}	8.403×10^{-11}	$2.142 \times 10^{+00}$
	38	87	0.51641	0.51643	2.146×10^{-08}	5.882×10^{-11}	7.376×10^{-01}
	41	93	0.84950	0.84931	6.536×10^{-09}	3.802×10^{-11}	8.194×10^{-03}
	43	99	1.11697	1.11672	3.448×10^{-09}	2.967×10^{-11}	5.277×10^{-03}
	49	113	2.10110	2.10055	8.000×10^{-10}	1.577×10^{-11}	1.184×10^{-03}
	49	115	2.10110	2.10055	8.000×10^{-10}	1.577×10^{-11}	1.179×10^{-03}
	72	179	6.80490	6.80544	6.369×10^{-11}	1.786×10^{-12}	1.491×10^{-03}
	83	209	9.11260	9.10502	3.584×10^{-11}	5.848×10^{-13}	8.025×10^{-06}
	83	208	9.11260	9.10493	3.584×10^{-11}	5.848×10^{-13}	6.433×10^{-06}
5	57	138	3.67249	3.67170	2.304×10^{-10}	7.463×10^{-12}	5.069×10^{-04}
	83	208	9.11260	9.10493	3.584×10^{-11}	5.848×10^{-13}	6.433×10^{-06}
7	67	166	5.75836	5.75705	8.929×10^{-11}	2.915×10^{-12}	1.057×10^{-04}
	71	176	6.59569	6.59411	6.757×10^{-11}	1.972×10^{-12}	7.540×10^{-05}
9	73	180	7.01409	7.01193	5.988×10^{-11}	1.618×10^{-12}	2.501×10^{-05}
	83	210	9.11260	9.11009	3.584×10^{-11}	5.848×10^{-13}	2.003×10^{-05}